

# Laboratory Study of Contaminants Migration Pattern in Soil Using 2D Electrical Resistivity Tomography

Nur Atikah Mohd Ali, Umar Hamzah, Mohd Amir Asyraf Sulaiman

*Geology Programme, Universiti Kebangsaan Malaysia*

## Abstract

*Migration pattern of contaminants in soil such as by hydrocarbons and saltwater has long been studied. The contaminants might be originated from oil spills, leakage from underground storage tanks (UST) and saltwater intrusion. The electrical resistivity technique is oftenly been used to detect the contaminants' plume in the subsurface. To understand the nature of contaminants migration pattern, a small scale laboratory study was carried out by measuring LNAPL contaminants using mini electrodes electrical resistivity imaging. Semi-water saturated fine sand, coarse sand and clay were used as the medium in the study. Electrical resistivity imaging was performed in the third and seventh days after the release of LNAPL. Resistivity section shows clearly the positions of fresh water-saturated zones in the top and bottom layers with resistivity values of about 100-200  $\Omega m$ . The semi-saturated zone occupied the middle part of the section with resistivity ranges from 500-1500  $\Omega m$ . The shape and positions of contaminants in clay medium with 30% water content is much easily detected compared with its migration patterns in coarse sand.*

- Improper disposal or hazardous or other chemical wastes
- Recharge of groundwater with contaminated surface water

## 1.1. Characterization of NAPLs

Nonaqueous Phase Liquid (NAPL) is a chemical that are only sparingly soluble migrate through aquifer as a separate non aqueous phase (*i.e* hydrocarbons). NAPLs also does nothave homogeneity phase when contacted with water and air. Hydrocarbon elements bonded together by covalent bonds. These compounds exist as a gas, liquid or solid. Hydrocarbons can be classified into two main groups, aliphatic and benzene. Aliphatic had four small groups of alkanes, alkenes, alkynes and aliphatic ring. Differences in physical and chemical properties of water and hydrocarbons cause it can not be mixed because there are physical boundaries of the interface [1].

Hydrocarbon can be classified into Light Non Aqueous Phase Liquid (LNAPL) and Dense Non Aqueous Phase Liquid (DNAPL) [2]. LNAPLs such as gasoline, fuel oil and diesel are less dense than water and will tend to float on the water surface. Some of LNAPLs will dissolve into groundwater and adsorb to pore spaces of vadose zone. LNAPL head distribution controls the lateral migration [3]. While DNAPLs such as Perchloroethylene (PCE) and Trichloroethylene (TCE) are dense than water. They are tend to sink in the aquifer below water table. Therefore the remediations of DNAPLs leakage and spills is quiet difficult. Today, most of the spills and leakage are hydrocarbons LNAPL and the best method to detect the plume and the migration is using geoelectrical techniques. NAPLs contaminated soil can be characterized through electrical resistivity technique due to higher resistivity values of NAPLs compared to water. Various studies hasbeen proved that the hydrocarbon plumes give higher resistivity anomaly [4-6]. Flow of the NAPLs are dependent upon viscosities, densities, interfacial tension of the

## 1. Introduction

Measurement of contaminant migration patterns are becoming increasingly important in a rapidly growing developing countries because of the increasing pollution of groundwater every year. Groundwater contamination will ultimately influence the groundwater system due to several factors. Two major source of contaminants are saltwater intrusion and uncontrolled releases of biological and chemical contaminants :

- Leaking Underground LNAPL Storage Tanks (UST)
- Leaking landfills

liquids, hydraulic permeability, water content of porous medium, and capillary forces. Low density and high viscosity contaminants tend to migrate horizontally and vertically due to gravity force.

## 1.2. Background

Over the past few years, various geophysical studies have shown the possibility to use Electrical Resistivity Tomography (ERT) to study the resistivity distribution of hydrocarbon contaminated soil [7], leachate leaking from a landfill [8,9], monitor plume segment movement [10] and saltwater intrusion [11]. Since contaminants and groundwater has large differences in resistivity variations, electrical resistivity method is useful for monitoring and detecting the contaminants plume in porous medium and rocks [12]. Besides, this method offers non-destructive, low cost, easy visualization-measurement manner and non-radiation.

## 2. Materials And Method

### 2.1. Inverse modelling

RES2DINV software is designed to invert large amount of data collected by set of electrodes system. The size and distribution of the model consists two-dimensional (2D) rectangular blocks are automatically generated. The depth of the model depends on the electrode spacing was used. For Wenner configuration, the first block layer thickness was set at 0.5 times of electrode spacing.

Generally, blue for low resistivity zone while red for high resistivity zone.

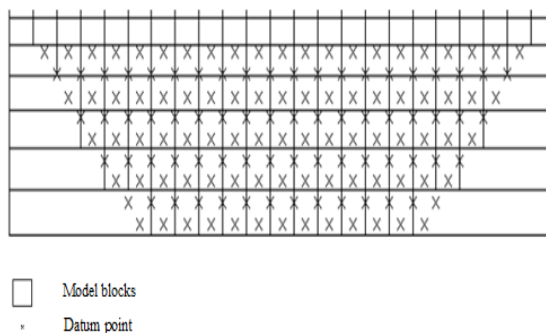


**Figure 1. The arrangement of blocks and data points in pseudosection**

These blocks (Fig. 1) will be colored according to the measured resistivity values by the system.

RES2DINV software is designed to produce the inverse model resembling the actual subsurface structure [13]. Resistivity data collected from the field gives the image as the sub-surface. Inversion routine used in RES2DINV is based on least-square method [14] written as :

$$(J^T J + uF)d = J^T g \quad (1)$$

where  $F$  denotes for  $f_x f_x^T + f_z f_z^T$ ,  $f_x$  the horizontal flatness filter,  $f_z$  the vertical flatness filter,  $J$  the matrix of partial derivative,  $u$  the damping factor,  $d$  the perturbation vector model and  $g$  the discrepancy vector.

### 2.2. Preparation of the experimental models

This study were conducted at normal gravity,  $1g$  ( $9.81 \text{ ms}^{-2}$ ) in room temperature. The porosity of coarse silica sand and fine silica sand are 0.45 and 0.38 respectively while porosity for clay is lower than both silica sand. A model of coarse silica sand has been partially saturated homogeneously with 5% water content and filled into the  $0.2\text{m} \times 0.1\text{m} \times 0.4\text{m}$  strongbox. After 1 day, the 100mL dyed diesel (dyed with Sudan V) used as a contaminant were released just about the center of the center of the model's surface (Fig. 2) and the point was marked and measured from left and right side. This steps will be repeated for fine silica sand and clay with different percentage of water content and contaminants (Engine oil and NaCl). Engine oil, diesel and NaCl were chosen as contaminant due to their densities and viscosities.



**Figure 2. Releasing dyed LNAPL**

### 2.3. Measurement of Electrical Resistivity

Migration pattern of the contaminants are observed both visually and the ERT method. ERT

method is used to detect the contaminant's plume in partially saturated porous media. On the third day, an electrode arrays (Fig.3) consisted of 41 multi mini electrodes with 8 mm long and 1cm apart between electrodes were installed horizontally along the centreline of the the strongbox. Those mini electrodes were connected to Electrode Selector ES464 and ABEM Terrameter SAS 1000 using crocodile clips and cables. A Wenner configuration was used in this study because time limitation and it is less sensitive than other geometry arrays. This measurement was carried out every third day and seventh day and data being recorded.

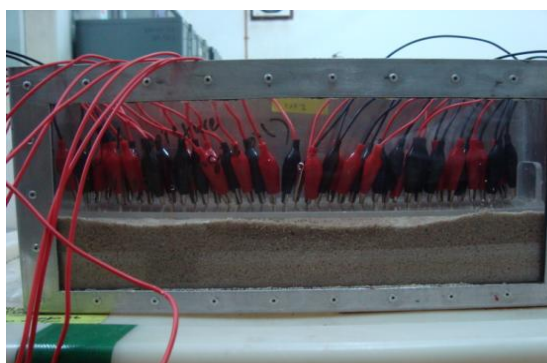


**Figure 3. The electrodes array were installed along the centreline of the model**

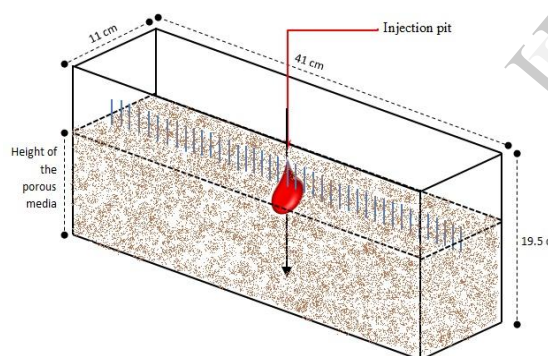


**Figure 4. Synthetic model**

## 2.4. Data processing and analysis

Raw data will be recorded and transferred to computer in '.dat' extension to plot two dimension (2D) pseudosection model image. RES2DINV software were used to invert all the resistivity measurements [15]. The software is able to interpret the raw data by selecting an optimal inverse parameters automatically according to specific data sets [16]. However, users still can change the

parameter because the algorithm to correct the image resolution, resistivity contrast and model depth variation may not be accurate. The apparent resistivity is translated in the form of contour color, generally blue for low resistivity zone while red for higher resistivity zone. The zone depends on the anomaly of the study area. In this study, the minimum electrode spacing on the instrument ABEM Terrameter SAS 1000 can be adjusted only to 0.1m which is 10 times larger than the actual electrode spacing in this experimental setup. Thus, to get accurate, each apparent resistivity values,  $\rho$  in raw data have been modified by dividing all values by 10. The generated resistivity inverse models will be interpreted and compared according to time and the mobility parameters ; porosity and water content of porous medium and viscosity of contaminants. Besides, the models also have been compared to visual observation through one side strongbox wall for accuracy.

## 3. Results And Discussion

### 3.1. Time-lapse Analysis

The ERT results of the tank model show resistivity variation from top to bottom. Fig. 5 shows the resistivity model of coarse silica sand saturated with 5% water content without contaminant measured after three days . This contaminant-free model is used for comparison with the contaminated model. While Fig. 6 and Fig. 7 are resistivity models using NaCl solution as contaminant. Resistivity measurements were made three and seven days after mixing the NaCl solution with the sand. Fig. 6 represents resistivity measurement after three days and Fig. 7 representing resistivity measurement after seven days of the mixing. The arrow indicates the point of contaminant release. The position of the NaCl solution is clearly observed in Fig. 6 and Fig. 7 as represented by the very low resistivity value zones of 1 - 8  $\Omega m$  spotted in the middle below the arrow and in small zones in the left and right part of the model. The seventh day resistivity model shows almost similar pattern where the NaCl plume concentrated below the released point. This contaminated model are very much in different than the uncontaminated one where the resistivity range of the uncontaminated model is from 80  $\Omega m$  to 1400  $\Omega m$  interpreted as representing water-saturated and semi-saturated coarse sand. The water-saturated zone has resistivity value of about 80  $\Omega m$  to 200  $\Omega m$  while the semi-saturated zone



represented by resistivity values of about 900  $\Omega\text{m}$  to 1400  $\Omega\text{m}$ .

Resistivity model of the uncontaminated sand measured after third day shows high resistivity about 1355  $\Omega\text{m}$  corresponding to the dry sand. This is due to the interstitial water settled into the base of the box. The position of the high resistivity of dry

sand are shown by the arrow on the left of the box due to inhomogeneity of the coarse sand. Zone of highly water-saturated are scattered in the box as shown by the arrow. This wet zone has resistivity values between 100  $\Omega\text{m}$  to 200  $\Omega\text{m}$  located mostly in the bottom part of the box.

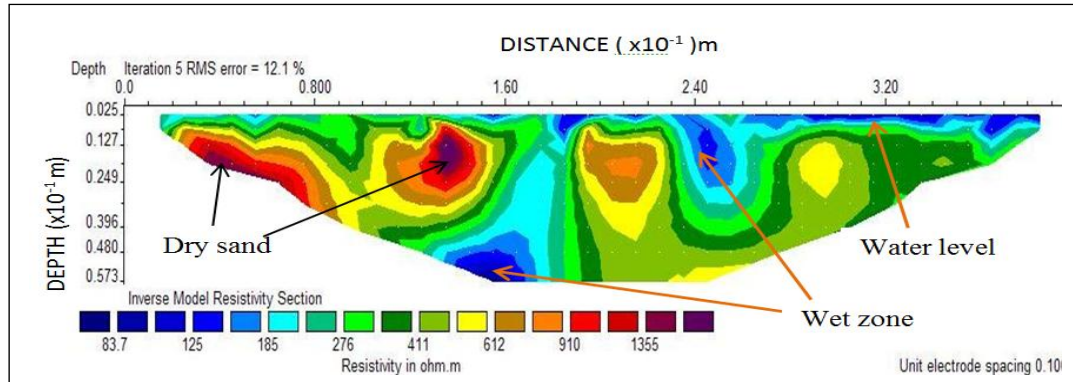


**Figure5. ERT result, coarse silica sand, 5% water content, no contaminant released, day 3 (controlling model)**

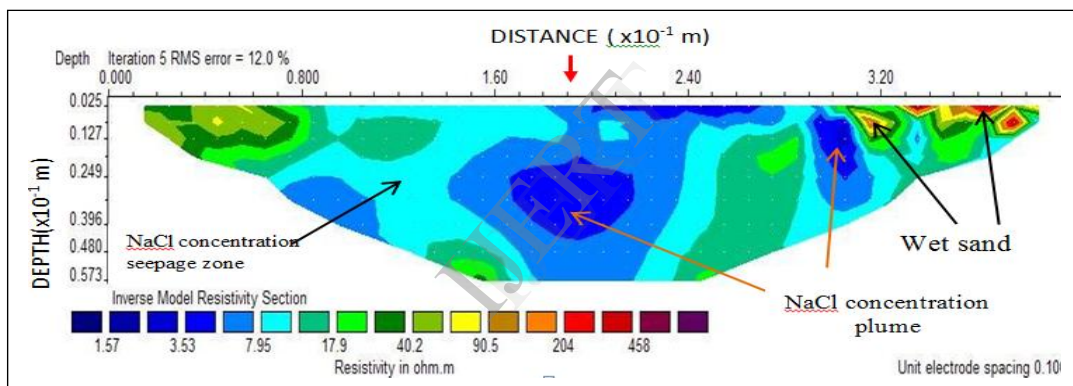


**Figure6. ERT result, coarse silica sand, 5% water content, NaCl concentration as the contaminant (3rd day)**

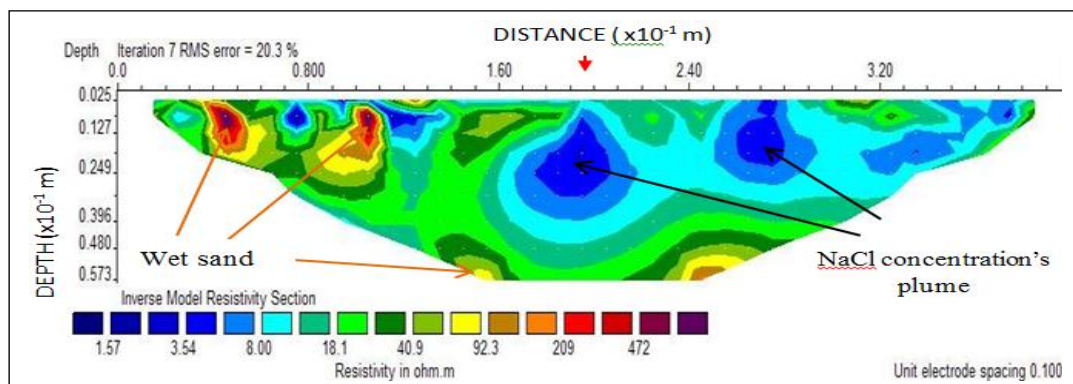


**Figure7. ERT result, coarse silica sand, 5% water content, NaCl concentration as the contaminant (7th day)**

### 3.2. The effect of water content of LNAPL migration

Experiment were carried out to investigate the migration pattern of different type LNAPL with different water content in coarse grain silica sand. Fig. 8 shows the migration pattern of diesel in coarse sand containing 5% water content by weight measured after seven days of the contamination and Fig. 9 shows same contaminant and time-lapse but with 15% water content. Both Fig. 8 and Fig. 9 indicate very low resistivity zone at the base of the boxes corresponding to highly saturated water zone about 20  $\Omega\text{m}$  to 100  $\Omega\text{m}$ .

In both figures, the position of highly contaminated zone are shown by the highest resistivity values. The diesel plume in 5% water content shows resistivity values of about 13000  $\Omega\text{m}$

to 15000  $\Omega\text{m}$  whereas the highly contaminated zone in the 15% water content box is about only 1000  $\Omega\text{m}$  to 2000  $\Omega\text{m}$ . The difference in the resistivity values can be interpreted due to the different in water content. In terms of diesel migration, the diesel spread into a much larger area (Fig. 8) in the drier sand whereas the diesel plume concentrated only in a middle part of the box for the higher water content sample as shown in Fig. 9.

The position of the contaminant plumes in both tests were located above the water saturated zone mainly due to the less dense of the diesel compared to water. The contaminated zone is produced by migration of LNAPL's vapors and therefore the vapors will move faster in the much drier sand [17].

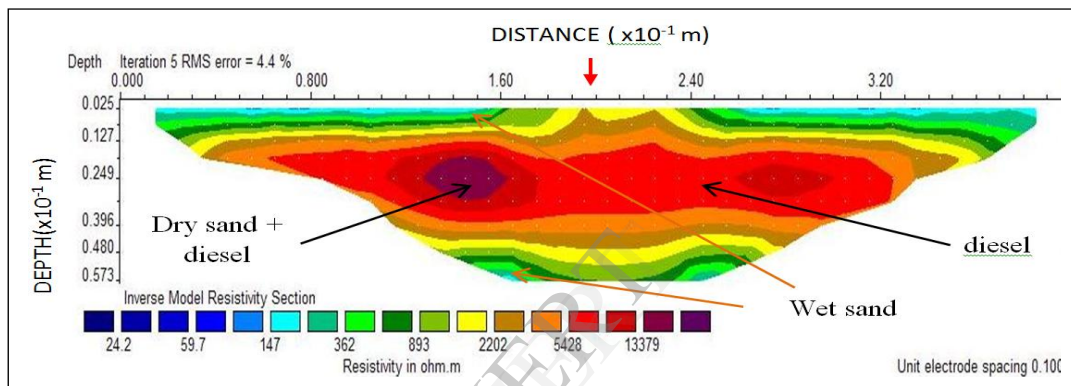


Figure8. ERT result, coarse silica sand, 5% water content, diesel as contaminant (7th day)

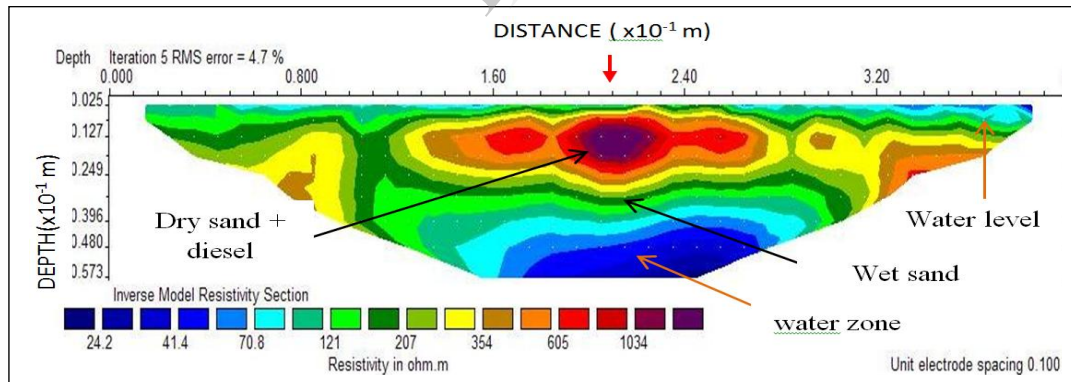


Figure9. ERT result, coarse silica sand, 15% water content, diesel as contaminant (7th day)

### 3.3. The migration pattern of different type of LNAPL in coarse sand

For this purpose diesel and engine oil type of LNAPL were used in the test. The medium used is coarse silica sand with 15% water content. Fig.

10 shows the migration pattern of engine oil in coarse silica sand with 15% water content after seven days of the LNAPL released while Fig. 11 shows the resistivity distribution pattern of diesel in coarse silica sand also with 15% water content. Based on the high resistivity plumes representing the engine oil and also the dry sand, the migration

of the engine oil could hardly be differentiated based on only the resistivity values. The engine oil plumes are estimated located near the release point. The same high resistivity values on the left and the right side of the box are interpreted as representing the dry sand and as usual the water are accumulated at the base of the box. The resistivity values of the engine oil are estimated in between 1000  $\Omega\text{m}$  to 2000  $\Omega\text{m}$ .

Fig. 11 shows the test for diesel where the maximum resistivities of about 1000  $\Omega\text{m}$  to 2000  $\Omega\text{m}$

$\Omega\text{m}$  was found located vertically below the release point. On top of the water saturated zone with 24  $\Omega\text{m}$  to 100  $\Omega\text{m}$  resistivity values. From this two tests the engine oil plume as travelled much deeper compared to the diesel plume due to much higher density of the engine oil compared to the lower density of diesel. After seven days of the released as travelled to a depth of about 4 cm from the surface of the soil. As for the diesel, the plume travelled only to about 2.5 cm from the surface.

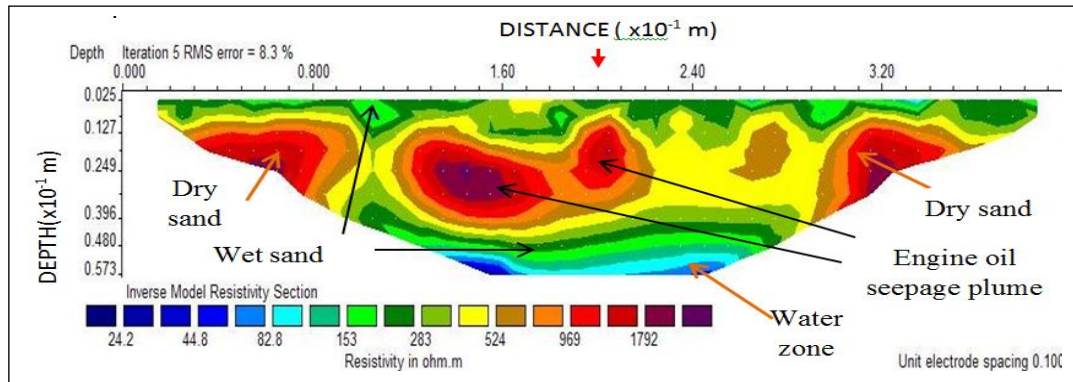


Figure 10. ERT result, coarse silica sand, 15% water content, engine oil as contaminant (7th day)

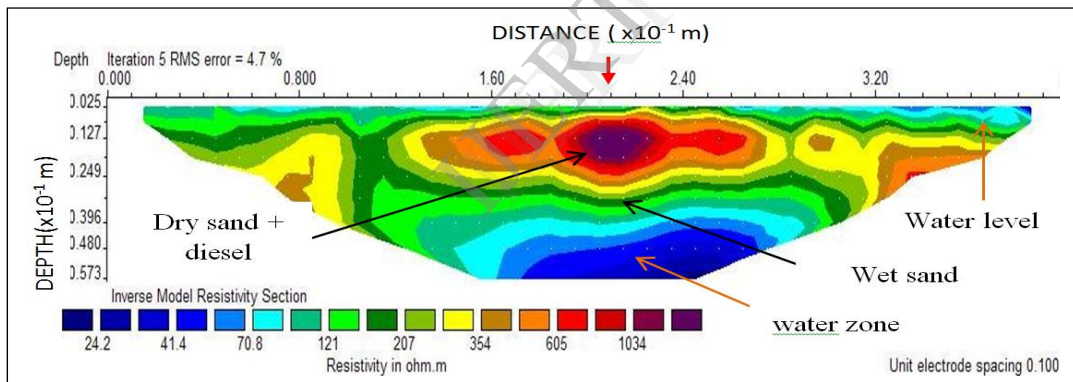


Figure 11. ERT result, coarse silica sand, 15% water content, diesel as contaminant (7th day)

### 3.4. Effect of grain size on the LNAPL migration

Since the mobility of LNAPL migration depends on the grain size of the media, several tests involving different LNAPL migrating into different sand and clay of different grain size were also tested. For this purpose, coarse and fine grain sand with porosity 0.45 and 0.28 respectively were used as the contamination media. For this test, the media is 15% saturated with brine solution and was homogenized for one day. As usual, after

homogenizing with the brine solution, engine oil is released in the middle of the box.

Fig. 12 shows the resistivity model of engine oil in fine silica sand with 15% NaCl measured seven days after the contamination. The lowest resistivity (0.03  $\Omega\text{m}$  to 1.5  $\Omega\text{m}$ ) appeared at the top of the resistivity model representing mostly brine saturated sand. Underlain this layer is much higher resistivity layers with resistivity of 300  $\Omega\text{m}$  to 13000  $\Omega\text{m}$  corresponding to the settlement of the engine oil right to the bottom of the test box. However the engine oil migration in the coarse sand shows a slightly different pattern than of the pattern in the fine sand.



The pattern is shown in Fig. 13 where the resistivity high of the oil zone can be trace right from the release point until the bottom of the box with resistivity values ranging from 300  $\Omega\text{m}$  to 10000  $\Omega\text{m}$ . For the coarse silica sand medium, the

low resistivity zone corresponding to the brine saturated zone is deeper than in the fine silica sand media. The thicker low resistivity layers is due to the easier path for the brine migration because of the bigger pore space of the silica sand.

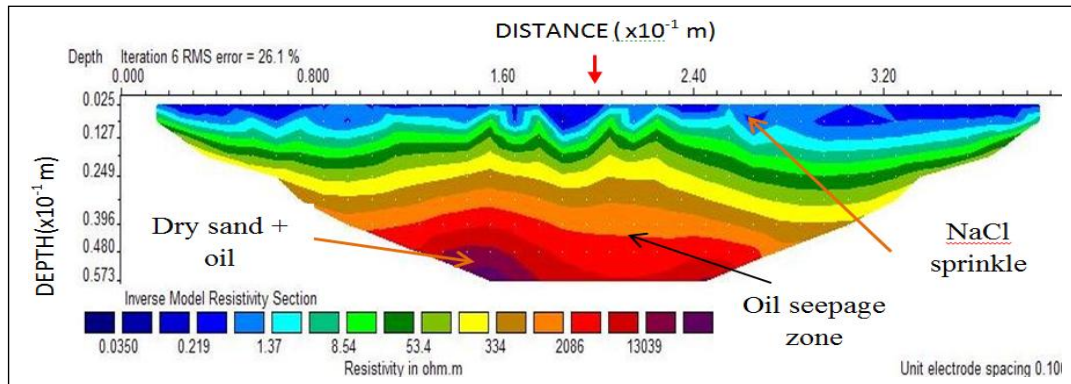


Figure 12. ERT result, fine silica sand, 15% NaCl water content, engine oil as contaminant (7th day)

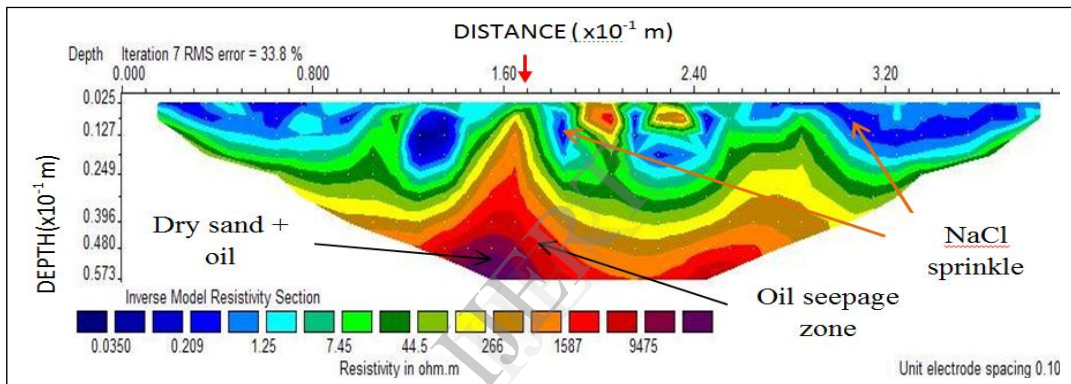
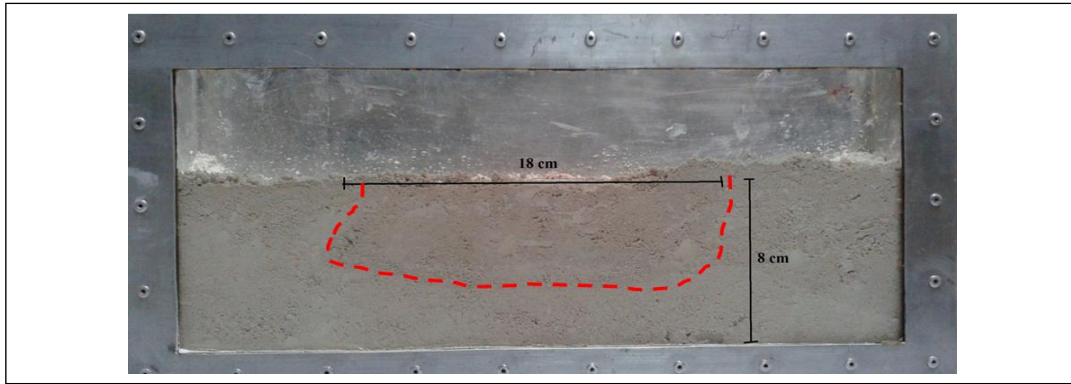


Figure 13. ERT result, coarse silica sand, 15% NaCl water content, engine oil as contaminant (7th day)

### 3.5. The effect of clay medium to the different LNAPL migration

Engine oil and diesel movement in clay were also investigated in the laboratory. Prior to the contamination, the clay was homogenized with 30% of water. Fig. 14 shows the photograph of diesel after seven days of its released. The diesel plume is clearly observed in the perspex box as delineated by the dash line. The resistivity model obtained after seven days of the contamination is shown in Fig. 15. The electrical resistivity tomography clearly indicates the oval shape corresponding to the diesel saturated zone with resistivity value as high as about 14000  $\Omega\text{m}$ . The dimension of the plume in both resistivity models and the test box are quite similar indicating the 2D resistivity technique managed as successfully

delineated the plume. The upper part of the resistivity model was occupied by low resistivity patches of low resistivity values representing wet clay of 6  $\Omega\text{m}$  to 60  $\Omega\text{m}$ .



**Figure14. Visual observation of diesel migration in 30% water content clay (7th day)**

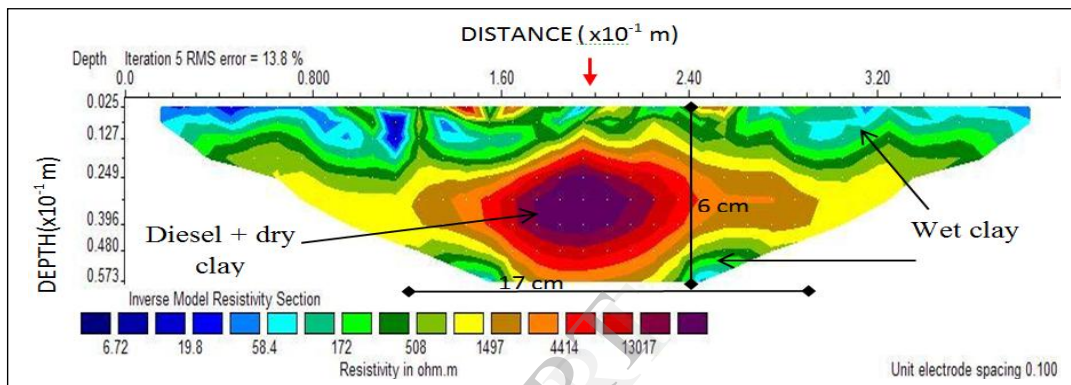


**Figure15. ERT result, clay, 30% water content, diesel as contaminant (7th day)**

In the next test, engine oil as the contaminant was released in the same clay medium. The photograph and the resistivity model for engine oil contamination are shown in Fig. 16 and Fig. 17. The dimension of the engine oil plume in the test box is 5 cm x 15 cm and the size of the contaminated zone interpreted as corresponding to the highest resistivity plume of about 2000  $\Omega$ m to 5000  $\Omega$ m is

observed in resistivity model. The engine oil was concentrated from top to about 5 cm depth below the released point. The length of the engine oil indicating the horizontal movement of the contaminant is about 17 cm.

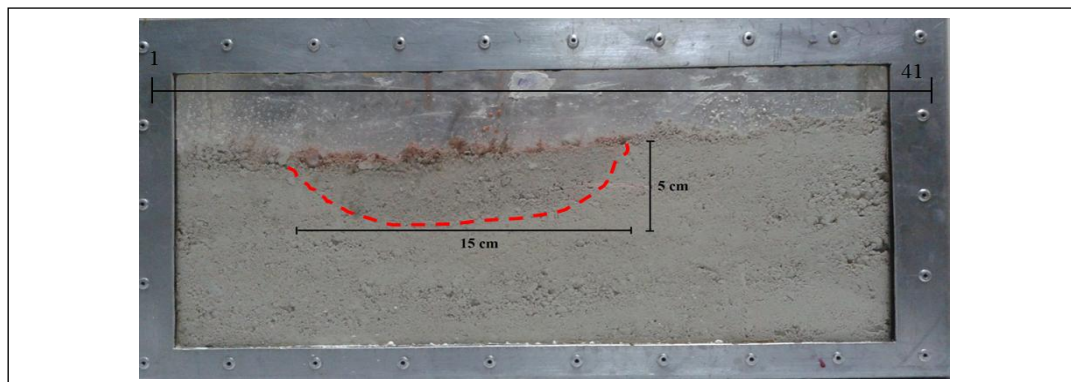


**Figure 16. Visual observation of engine oil migration in 30% water content clay (7th day)**



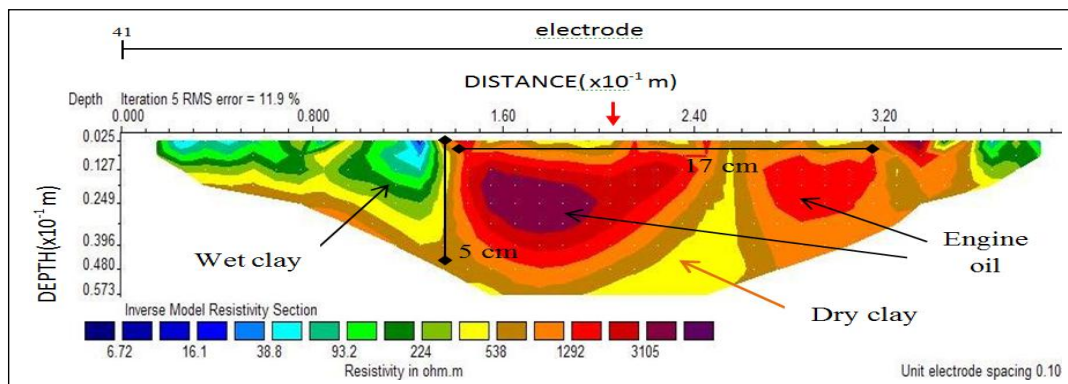


**Figure 17. ERT result, clay, 30% water content, engine oil as contaminant (7th day)**

The resistivity values of different LNAPL in different porous media are significantly different as observed in the laboratory test. Table 3.1, indicates

the resistivity values of different LNAPL in different media with different water content.

**Table 3.1 Characterization of resistivity for different LNAPLs with different water content in 7 days**

Media	Grain size	Water Content (%)	Resistivity of Contaminants ( $\Omega$ m)	
			Diesel	Engine Oil
Silica Sand	fine (40/80)	5	1000-10000	1000-10000
		15	800-5000	300-1300
	Coarse (16/30)	5	13000-15000	800-5000
		15	1000-2000	300-10000
Clay	7.0-11.0	30	1500-14000	2000-5000

Higher resistivity is observed in coarse silica sand with 5% water content compared with resistivity in coarse silica sand with 15% water content. This indicate drier silica sand with similar LNAPL shows higher resistivity values indicating the influence of water increasing the water conductivity in the sand medium. Secondly, the porosity of media also influenced the resistivity of same LNAPL with same water content. In this study, the resistivity of engine oil in coarse silica sand is about 800  $\Omega$ m to 5000 $\Omega$ m which is lower

compared to the resistivity in fine silica sand which is about 1000  $\Omega$ m to 10000  $\Omega$ m.

The resistivity of diesel observed in clay with 30% water content is between 1500  $\Omega$ m to 14000  $\Omega$ m which is higher than the resistivity of engine oil in the same medium and water content which is about 2000  $\Omega$ m to 5000  $\Omega$ m. The resistivity of these LNAPLs are slightly higher than their resistivity values in silica sand.

#### 4. Conclusion

In general, high resistivity values always associates with the presence of hydrocarbons either engine oil or diesel compared with resistivity of non-LNAPL media. The resistivity of diesel is found much higher compared to the resistivity

values of engine oil in clay with same water content. The resistivity of diesel also is found much higher compared to the resistivity of engine oil in both fine and coarse silica sand. The resistivity of diesel or engine oil is always much higher in lower water content than in the higher water content.

## References

- [1] Chiswell B. & James D.W. 1981. *Aspek Asas Kimia Tak Organik*. Kuala Lumpur. Dewan Bahasa dan Pustaka.
- [2] Tan Chin Lee. 2007. Keberkesanan kaedah keberintangan geoelektrik dalam kajian rerongga dan pencemaran LNAPL bawah permukaan. Tesis Sarjana Sains. Universiti Kebangsaan Malaysia
- [3] Newell, C.J., Acree, S.D., et. al., 1995, Ground Water Issue : Light Nonaqueous Phase Liquids, US Environmental Protection Agency, EPA/540/S-95/500.
- [4] Matias de la Vega et. al., 2003, Joint inversion of Wenner and dipole-dipole data to study a gasoline-contaminated soil, *Journal of Applied Geophysics*, **54**(1-2), 97-109
- [5] G. Buselli & K. Lu, 2001, Groundwater contamination monitoring with multichannel electrical and electromagnetic methods, *Journal of Applied Geophysics*, **48**, 11-23
- [6] A.K. Benson, K.L. Payne & M.A. Stubben, 1997, Mapping groundwater contamination using dc resistivity and VLF geophysical methods., *Geophysics*, **62**, 80-86
- [7] Umar Hamzah, Mohd Azmi Ismail & Abdul Rahim Samsudin, 2009, Geoelectrical resistivity and ground penetrating radar techniques in the study of hydrocarbon-contaminated soil, *Sains Malaysiana*, **38**(3), 305-311
- [8] Lorenzo De Carlo et. al., 2013, Characterization of a dismissed landfill via electrical resistivity tomography and mise-à-la-masse method, *Journal of Applied Geophysics*, **98**, 1-10
- [9] Joseph T. Zume et. al. , 2006, Subsurface Imaging of an Abandoned Solid Waste Landfill Site in Norman, Oklahoma, *Groundwater Monitoring & Remediation* , **26**(2), 62-69
- [10] P. Vaudelet et. al., 2011, Mapping of contaminant plumes with geoelectrical methods. A case study in urban context , *Journal of Applied Geophysics*, **75** (4), 738-751
- [11] R. de Franco<sup>a</sup> & G. Gasparetto-Stori<sup>h</sup> , 2009, Monitoring the saltwater intrusion by time lapse electrical resistivity tomography: The Chioggia test site (Venice Lagoon, Italy) , *Journal of Applied Geophysics* , **69**(3-4), 117-130
- [12] Schneider G.W & Greenhouse J.P, 1992, Geophysical detection of perchloroethylene in a sandy aquifer using resistivity and nuclear logging technique, *Proceedings of the symposium on the application of geophysics to engineering and environmental problems*, EEGS, 619-628
- [13] M.H Loke, Acworth, I. and Dahlin, T., 2003, A comparison of smooth and blocky inversion methods in 2D electrical imaging surveys, *Exploration Geophysics*, **34**, 182-187
- [14] deGroot-Hedlin, C. & Constable, S., 1990, Occam's inversion to generate smooth, two-dimensional models form magnetotelluric data, *Geophysics*, **55**, 1613-1624
- [15] M.H Loke & R.D. Barker, 1995, Improvements to the Zohdy method for the inversion of resistivity sounding and pseudosection, *Computers & Geosciences*, **21**(2), 321-332
- [16] M.H Loke, 1997. Electrical imaging surveys for environment & engineering studies, *School of Physics*, Universiti Sains Malaysia.
- [17] Mendoza, C.A & T.A. McAlary, 1989, Modeling of groundwater contamination caused by organic solvent vapors, *Ground Water*, **28**(2), 199-206